Hypochlorous Acid Decomposition in the pH 5–8 Region

Luke C. Adam, István Fábián,† Kazunori Suzuki, and Gilbert Gordon*

Department of Chemistry, Miami University, Oxford, Ohio 45056

Received October 23, 1991

The decomposition of hypochlorous acid in the neutral pH region was studied in 1.0 M $NaClO_4$ from 15 to 50 °C. The pK_a of HOCl was also determined under these conditions. Hypochlorous acid has a maximum decomposition rate at pH 6.89. The decomposition is a third-order process. The values of $\Delta H^{\ddagger}$ and $\Delta S^{\ddagger}$ are 64.0 ± 0.6 kJ/mol and −67 ± 2 J/mol K, respectively. A mechanism for the decomposition of HOCl is proposed involving $Cl_2O{\cdot}H_2O$ and ClO_2^- as intermediates. Rate constants for the rate-determining steps of the mechanism are presented. Above pH 6, the rate-determining step is proposed to be as follows: $OCl^- + Cl_2O{\cdot}H_2O \rightarrow HCl_2O_2^- + HOCl$. Below pH 6, this process is proposed to be in competition with a parallel pathway: $HOCl + Cl_2O{\cdot}H_2O \rightarrow H_2Cl_2O_2 + HOCl$. The proposed mechanism was tested by mathematical simulation of the experimental data using the GEAR algorithm. The simulation gives additional support for the proposed mechanism.

Introduction

The decomposition of hypochlorous[1] acid ($HOCl + OCl^-$) has been studied by Chapin[2] from pH 1 to pH 13. This work shows a maximum decomposition rate in the neutral pH range. The following stoichiometry and rate law was found to approximate the experimental observations:

$$2HOCl + OCl^- \rightarrow ClO_3^- + 2H^+ + 2Cl^- \quad (1)$$

$$-d[HOCl]/3dt = k[HOCl]^2[OCl^-] \quad (2)$$

This work is not considered to give quantitative rate constants due to the fact that the measurements were not carried out at constant ionic strength and only five data points were collected vs time for each experiment. Also, the experiments were carried out in potentially interfering phosphate buffer solution.

The decomposition of hypochlorous acid was also studied by Yokoyama and Takayasu[3] in the neutral pH region. Their work was carried out in 0.8–4.6 M chloride ion to control the ionic strength, and no buffer was used. They found that their experimental data was best approximated by the following rate law:

$$-d[HOCl]/3dt = a[HOCl]^2[OCl^-]/(1 + b[OCl^-]) \quad (3)$$

In eq 3, a and b are constants. When $b[OCl^-] \ll 1$, eq 3 simplifies to eq 2. The denominator in eq 3 takes into account the experimentally observed order of 0.85 with respect to OCl^- for the decomposition. As the concentration of OCl^- decreased from 0.18 to 0.06 M during the course of the decomposition, the order was found to approach 1.0. The authors proposed the following mechanism for the decomposition of hypochlorous acid:

$$HOCl + HOCl \rightarrow H_2Cl_2O_2 \quad (4)$$

$$H_2Cl_2O_2 + OCl^- \rightarrow ClO_3^- + 2H^+ + 2Cl^- \quad (5)$$

$$OCl^- + H^+ = HOCl \quad (6)$$

The intermediate in eq 4 is a proposed dimer of HOCl. While this mechanism agrees with the rate law in eq 2, it cannot explain the experimentally observed rate expression in eq 3.

In the present work, a detailed study of the decomposition of hypochlorous acid is presented from pH 5.0 to pH 8.0. Sodium hypochlorite (NaOCl) of the highest purity was prepared for this work. Also, the ionic strength of the decomposing hypochlorous acid solutions was controlled by $NaClO_4$. No buffers were added to these solutions except where the effect of buffers were studied specifically.

Experimental Section

Reagents. All solutions were prepared using deionized triply distilled water which was prepared by using a Barnstead/NANOpure water purification system. The resulting water was of highest quality that had no measurable chlorine demand. Pure sodium hypochlorite was prepared by a method similar to that used by Nagypál, Peintler, and Epstein.[4] Gaseous chlorine (Matheson) was bubbled through an aqueous slurry of yellow HgO at room temperature. For every mole of Cl_2 dissolved in the slurry, 3 mol of HgO were added to provide an adequate excess. The slurry was mixed with a magnetic stirrer and Teflon stirring bar for 45 min at which time all of the Cl_2 had been converted to HOCl and all of the chloride ion (initially produced by Cl_2 hydrolysis) was precipitated as $HgCl_2$. This $HOCl/HgCl_2/HgO$ slurry was distilled under a reduced-pressure nitrogen atmosphere into a 0.1 M NaOH solution, and the HOCl was collected as NaOCl. The nitrogen atmosphere was utilized so that no CO_2 would be present to form carbonate ion as a contaminant in the final NaOCl solution.

The flask used to contain the stock NaOCl solution was equipped with a ground glass filter tube containing soda lime to absorb any CO_2 from the air that enters the flask when a aliquot is removed from a separate outlet. All stock NaOCl solutions were stored in the dark at 5 °C and were used within 10 days of their production.

The stock solutions were checked for chloride ion contamination by acidifying an aliquot of stock NaOCl with dilute sulfuric acid and by adding 0.5 M $AgNO_3$. The absence of chloride ion ($\leq 4 \times 10^{-5}$ M) is indicated by no immediate precipitation of AgCl. Sodium hypochlorite concentrations up to 0.1 M were routinely obtained by this method and diluted to 0.05 M when stored in order to minimize the rate of decomposition. Stock NaOCl solutions were standardized by iodometric[5,6] titration. The excess NaOH concentration present in these solutions was determined by pH titration with standard HCl.

† On leave from the Institute of Inorganic and Analytical Chemistry, Kossuth L. University, Debrecen, Hungary.

(1) For the purposes of this paper, the term "hypochlorous acid" will be used to refer to the sum of the HOCl and OCl^- species.

(2) Chapin, R. M. *J. Am. Chem. Soc.* **1934**, *56*, 2211–2215.

(3) Yokoyama, T.; Takayasu, O. *Kogyo Kagaku Zasshi* **1967**, *70*, 1619–1624.

(4) Nagypál, I.; Peintler, G.; Epstein, I. R. *J. Phys. Chem.* **1990**, *94*, 2954–2958.

(5) Cady, G. H. In *Inorganic Synthesis*; Moeller, T., Ed.; McGraw-Hill Co.: New York, 1957; Vol. 5, pp 156–165.

(6) Gordon, G.; Cooper, W. J.; Rice, R. G.; Pacey, G. E. *Disinfectant Residual Measurement Methods*; (American Water Works Association Research Foundation): Denver, CO, 1987; pp 9–10, 53–55 (ISBN 0-89867-408-5).

0020-1669/92/1331-3534$03.00/0

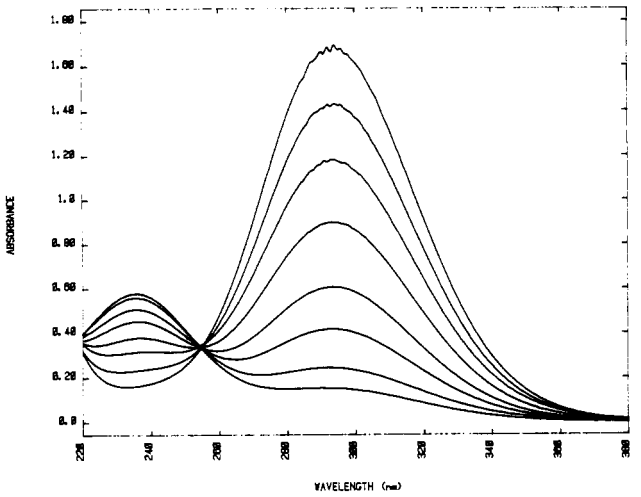

Figure 1. Spectra of HOCl and OCl^- vs pH for 4.8 mM hypochlorous acid in a 1-cm cell (50 °C). The OCl^- peak at 292 nm decreases with decreasing pH while the HOCl peak at 236 nm increases with decreasing pH. The pH values are as follows: 6.15, 6.55, 6.81, 7.09, 7.31, 7.62, 7.98, and 9.10.

Stock solutions of $NaClO_4$ were prepared by triply recrystallizing[7] freshly prepared solutions of $NaClO_4$ from $HClO_4$ and Na_2CO_3. The concentration of $NaClO_4$ was determined by drying a known volume in an oven at 120 °C and weighing the mass of the recovered solid. The NaOH that was used for all experiments was obtained by dilution of a nearly saturated stock NaOH solution that had been previously vacuum filtered to remove any precipitated Na_2CO_3. Unless stated otherwise, all other solutions were prepared directly from ACS reagent grade chemicals.

The final solutions for the decomposition measurements were prepared by adding predetermined amounts of NaOCl, $HClO_4$, and $NaClO_4$ to a beaker while stirring continuously. Each reagent was added with individual automatic titrators accurate to better than 0.01 cm^3 to provide a maximum dilution error of 0.13% in the final solution.

Instrumentation. Potentiometric titrations were carried out with a Radiometer ABU93 Triburette autoburette station connected to a Radiometer VIT90 Video Titrator unit. Iodometric titrations were carried out on this unit using a standard P101 platinum K401 SCE electrode pair by Radiometer. The same titrator unit was used for pH titrations with a Radiometer GK2401B combination glass electrode. Also, this combined glass electrode was used in conjunction with a Radiometer PHM64 pH meter for all pH measurements. The electrodes were calibrated such that the pH meter reading gave the hydrogen ion concentration (–log $[H^+]$), after the addition of a correction factor. A typical calibration involved the use of standard pH 4 and pH 7 buffers (Fisher) to first establish a linear response in this pH region. The response of standardized 0.01 M $HClO_4$ in 1.0 M $NaClO_4$ was then determined. The deviation in the pH reading obtained from the theoretical value of 2 was taken as the correction factor for the liquid junction potential of 1.0 M $NaClO_4$. Typical correction factors were near +0.27 pH units.

Accurate amounts of stock reagents for the decomposition experiments were added using Metrohm Herisau Dosimat E535 and Multi-Dosimat E415 automatic titrators. The Radiometer ABU93 Triburette autoburette station was also used for this purpose. Except where flow injection analysis (FIA) was used, all spectrophotometric measurements were made with a Hewlett-Packard 8450 UV/vis diode array spectrophotometer. During decomposition experiments, temperature baths by Forma Scientific Inc. were employed. The temperature of the 1-cm quartz cell used was controlled by a hollow brass cell holder connected to the temperature bath. The cell was sealed with a tightly fitting ground glass stopper with no head space. The neck and stopper was wrapped with Parafilm and the characteristic odor of volatile HOCl could not be detected above the cell during the experiments. Losses of the volatile HOCl during mixing and transfer to the cell were found to be less than 1% by comparing the calculated value from the first absorbance spectrum with the theoretical value obtained by taking into account dilution of the standard stock NaOCl.

Flow injection analysis was carried out for the determination of chlorite and chlorate ion[8,9] as hypochlorous acid decomposition products with a Tecator FIAstar 5020 Analyzer coupled to a Tecator 5032 Controller unit.

For measurements involving ≥0.1 M initial HOCl concentration, a reaction vessel with a tightly fitting Teflon cap was used. The concentration of HOCl and ClO_2^- were determined iodometrically at pH 2 and the concentration of ClO_2^- was determined iodometrically after the selective reduction of HOCl with S(IV) under appropriate conditions.[10]

Table I. Data for the Calculation of pK_a of HOCl from 15 to 50 °C in 1.0 M $NaClO_4$[a]

$[H^+]$ (M)	absorbance	C^t_{HOCl} (M)	pK_a	
1.986E–07	0.867	8.997E–03	7.261	
9.705E–08	1.179	7.303E–03	7.159	
8.570E–08	1.064	6.397E–03	7.186	
7.161E–08	1.023	5.699E–03	7.193	
6.081E–08	0.994	5.007E–03	7.162	
av[b] (50 °C)			7.192	± 0.041
1.274E–07	1.068	8.997E–03	7.298	
8.995E–08	1.045	7.303E–03	7.299	
1.660E–07	0.666	6.370E–03	7.281	
3.750E–08	1.219	5.699E–03	7.294	
3.034E–08	1.162	5.007E–03	7.284	
av (40 °C)			7.291	± 0.008
1.318E–07	1.053	8.996E–03	7.295	
1.047E–07	0.958	7.291E–03	7.304	
5.943E–08	1.112	6.396E–03	7.310	
4.325E–08	1.139	5.698E–03	7.309	
1.671E–07	0.962	9.498E–03	7.304	
av (35 °C)			7.304	± 0.006
1.349E–07	0.740	7.303E–03	7.400	
4.140E–07	0.408	7.296E–03	7.392	
1.079E–07	0.739	6.400E–03	7.397	
7.295E–08	0.807	5.695E–03	7.403	
4.977E–08	0.855	4.999E–03	7.406	
av (25 °C)			7.400	± 0.005
1.368E–07	0.887	9.003E–03	7.419	
1.274E–07	0.757	7.303E–03	7.411	
1.028E–07	0.730	6.400E–03	7.431	
6.501E–08	0.807	5.695E–03	7.457	
4.529E–08	0.854	4.999E–03	7.452	
av (15 °C)			7.434	± 0.020

[a] Conditions: 292 nm, 1-cm cell, ϵ_{OCl^-} = 351 M^{-1} cm^{-1}, and ϵ_{HOCl} = 100 M^{-1} cm^{-1}. [b] The uncertainties represent 1 standard deviation.

Results and Discussion

pK_a Measurements. All measurements were carried out in 1.0 M $NaClO_4$ and at 50 °C unless stated otherwise. The species HOCl and OCl^- absorb in the 220–380-nm region and have absorbance maxima at 236 and 292 nm, respectively. The HOCl species has a broad shoulder absorbance around 290 nm. Measuring the absorbance at 292 nm where both HOCl and OCl^- absorb significantly and knowing the total concentration of both species allowed the pH of each HOCl solution prepared to be calculated directly. An accurate value for the pK_a of HOCl is essential for the pH calculation. The pH dependence of the absorbance spectrum for HOCl and OCl^- is given in Figure 1.

The pK_a was determined in 1.0 M $NaClO_4$ at five different temperatures. The determination was carried out by mixing predetermined quantities of NaOCl, $HClO_4$, and $NaClO_4$ standard stock solutions and measuring the absorbance spectrum and pH of the resulting $HOCl/OCl^-$ solution. Results of the pK_a determination are given in Table I.

(7) Gordon, G.; Tewari, P. H. *J. Phys. Chem.* **1966**, *70*, 200–204.

(8) Themelis, D. G.; Wood, D. W.; Gordon, G. *Anal. Chim. Acta* **1989**, *225*, 437–441.

(9) Wood, D. W. Determination of Disinfectant Residuals in Chlorine Dioxide Treated Water using Flow Injection Analysis. Ph.D. Dissertation, Miami University, Oxford, OH, 1990.

(10) Suzuki, K.; Gordon, G. *Anal. Chem.* **1978**, *50*, 1596–1597.

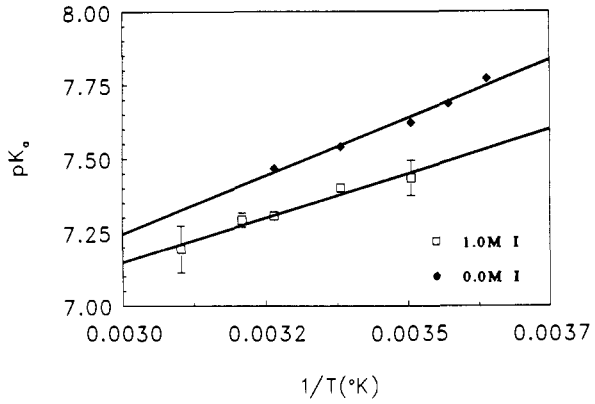

Figure 2. Plot of pK_a of HOCl vs temperature for zero[11] and one molar ionic strength (I) with $NaClO_4$ as the controlling electrolyte.

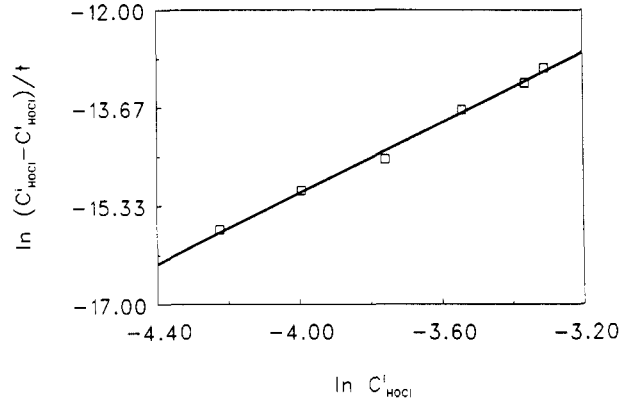

Figure 3. Plot of the ln of initial rate of total HOCl and OCl^- vs the ln of initial concentration for 5% decomposition at 50 °C and pH 7.1.

In Table I, the pK_a was calculated by using the following equation:

$$K_a = [H^+]\{(A/C^i_{HOCl}) - \epsilon_{HOCl}\}/\{\epsilon_{OCl^-} - (A/C^i_{HOCl})\} \quad (7)$$

Key: C^i_{HOCl}, total concentration of HOCl and OCl^- in the final solution before any decomposition has occurred; $[H^+]$, free hydrogen ion concentration from pH measurement; A, experimentally measured absorbance at 292 nm; ϵ_{HOCl}, molar absorptivity of hypochlorous acid at 292 nm; ϵ_{OCl^-}, molar absorptivity of sodium hypochlorite at 292 nm.

The pK_a values obtained are plotted vs temperature in Figure 2 along with pK_a data from Morris[11] at zero ionic strength for comparison. Both sets of data have similar slopes, and the pK_a values at one molar ionic strength are depressed by approximately 0.13 pK_a units in this temperature range.

The Eyring equation[12] was used to determine ΔH^* and ΔS^* of the HOCl equilibrium by plotting ln (K/T) vs $1/T$. The results are as follows: $\Delta H^* = 9.9 \pm 1.4$ kJ/mol; $\Delta S^* = -0.35 \pm 0.01$ kJ/mol K.

Kinetic Measurements. The absorbance of HOCl and OCl^- was followed as a function of time from 200 to 400 nm. Molar absorptivity values at the corresponding absorbance maxima were found to be in agreement with previous[11,13-15] determinations. The isosbestic point was determined to be at 254.7 nm in 1.0 M $NaClO_4$. By using the absorbance value at the isosbestic point, the total concentration of HOCl and OCl^- was determined as a function of decomposition time. The molar absorptivity at 254.7 nm was determined to be $57.1_3 \pm 0.6$ M^{-1} cm^{-1}.

Kinetic experiments were carried out at six different total HOCl and OCl^- concentrations at 50 °C and an initial pH of 7.09. In Figure 3, the natural log (ln) of the initial rate is plotted vs the ln of initial concentration of HOCl and OCl^-. The slope of this plot is $3.0_0 \pm 0.1_1$ and represents the overall order of the decomposition reaction.

According to our stoichiometric studies at 50 °C and pH 7.1, the ratio of hypochlorous acid reacted to chlorate ion formed is 2.91 ± 0.09 throughout the decomposition. This result indicates that there are no competing side reactions, and in accordance with previous literature,[2,3,16,17] the final products are ClO_3^- and Cl^- ions.

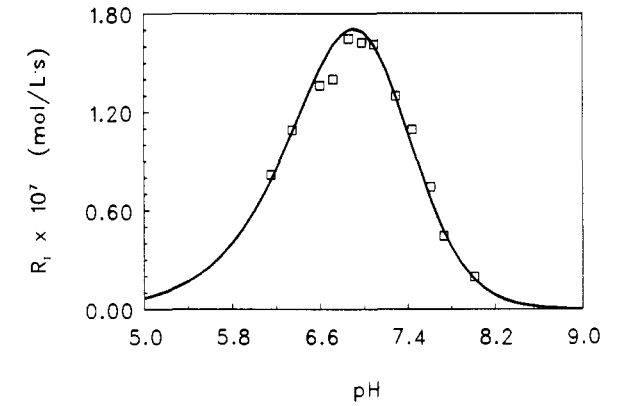

Figure 4. Plot of initial rate for 5% decomposition vs pH: (□) experimentally observed points; (—) generated curve. Conditions: $C^i_{HOCl} = 0.0233$ M, 50 °C, and $R_i = (C^i_{HOCl} - C^t_{HOCl})/3t$.

Experiments were carried out at 12 different hydrogen ion concentrations at constant total initial concentration of HOCl and OCl^-. The initial rate at 50 °C is plotted vs initial pH in Figure 4. The trend in the initial rate data vs pH followed a third-order rate law:

$$-d(C^i_{HOCl} - C^t_{HOCl})/3dt = k[HOCl]^2[OCl^-] \quad (8)$$

From $(C^i_{HOCl} - C^t_{HOCl})/3\Delta t$, the experimental rate constant was calculated for each experiment directly. The experimental rate constant was calculated to be 0.091 ± 0.006 M^{-2} s^{-1}. By using eq 8, the theoretical trend in the initial rate of decomposition was generated and is shown as the solid line in Figure 4. The kinetic experiment with the highest initial rate of decomposition corresponds to pH 6.86_2. By using the pK_a of 7.19_3 for HOCl, the theoretical rate maximum for this rate law should occur at pH 6.89_2.

The determination of the hypochlorous acid/ClO_3^- stoichiometry and the rate law in eq 8 results in the following stoichiometric equation for hypochlorous acid decomposition in the neutral pH region:

$$x\text{HOCl} + (3-x)\text{OCl}^- \rightarrow \text{ClO}_3^- + 2\text{Cl}^- + x\text{H}^+ \quad (9)$$

Consistent with eq 9, the pH of the decomposing hypochlorous acid solutions decreases vs reaction time and chloride ion can be detected by using silver nitrate. Both of these observations support the overall stoichiometry of hypochlorous acid decomposition.

A first-order plot of hypochlorous acid decomposition at an initial pH of 8.01 and 0.0233 M hypochlorous acid is strictly linear which suggests that the HOCl species concentration does not change appreciably. The pseudo-first-order rate law can be expressed as follows:

(11) Morris, J. C. *J. Phys. Chem.* **1966**, *70*, 3798–3805.
(12) Gordon, G.; Katakis, D. *Mechanisms of Inorganic Reactions*, Wiley-Interscience: New York, 1987; p 59.
(13) Soulard, M.; Bloc, F.; Hatterer, A. *J. Chem. Soc., Dalton Trans.* **1981**, *12*, 2300–2310.
(14) Silverman, R. A. Variation of Chlorine Hypochlorous Acid Equilibrium and Spectra with ionic strength; Kinetics and Mechanism of the Uranium(IV)–Hypochlorous Acid Reaction. Ph.D. Dissertation, University of Iowa, 1976, p 55.
(15) Silverman, R. A.; Gordon, G. *J. Phys. Chem.* **1980**, *84*, 625–629.
(16) Lister, M. W. *Can. J. Chem.* **1956**, *34*, 465–478.
(17) Lister, M. W. *Can. J. Chem.* **1956**, *34*, 479–488.

$$-d(C^{i}_{HOCl})/3dt = k'[OCl^-] \quad (10)$$

$$k' = k_{exp}[HOCl]^2 \quad (11)$$

Integrating eq 10 and making the appropriate substitutions, we obtained the following equation for the determination of k_{exp}:

$$k_{exp} = \frac{[1 + (K_a/[H^+])]^2[([H^+]/K_a) + 1]}{3(C^{i}_{HOCl})^2 t} \ln (A_0/A_t) \quad (12)$$

The value of k_{exp} obtained by this calculation is 0.091 ± 0.007 M^{-2} s^{-1}.

Figure 5 gives the concentration of total HOCl and OCl^- and the concentration of the HOCl species alone vs reaction time at an initial pH of 6.98. As the decomposition proceeds, the values of [HOCl] + [OCl^-] and [HOCl] eventually reach the same concentration since the hydrogen ions produced in the decomposition converts all of the OCl^- to HOCl. This figure also illustrates that the HOCl concentration does not change by more than 3% from its initial concentration throughout the measured decomposition range. This observation supports the pseudo-first-order condition for OCl^-.

Figure 6 is a first-order plot of absorbance of hypochlorous acid vs time for five different initial pH values. As the initial pH of the hypochlorous acid solutions becomes more acidic, the first-order plots become increasingly nonlinear and the nonlinearity begins at smaller percent decompositions. This is consistent with the fact that the HOCl species concentration begins to change appreciably as the acidity increases.

The experimentally observed deviation in first-order plots of the hypochlorous acid decomposition data appears to be due to the following. As the decomposition proceeds, the pH of the solution decreases and the deviation begins to occur near pH 6. Parallel pathways (i.e. rate-determining steps) with one path involving OCl^- and the other HOCl could explain the deviation. Above pH 6, the pathway involving OCl^- would have the greatest contribution to the decomposition while below this pH the hypochlorous acid would exist mainly as HOCl and a reaction path involving HOCl would compete with the OCl^- reaction path. At the point where the pH decreases below pH 6, the rate law would no longer be a simple third-order process and would become complex due to the competing parallel rate-determining steps. The estimation of the rate constants for these parallel rate-determining steps will be discussed later.

Decomposition measurements have also been carried out at 90 °C from pH 8 to pH 13 in 0.5 M borate buffer and in the absence of $NaClO_4$. The rate of hypochlorous acid decomposition and the formation of ClO_2^- is plotted vs pH in Figure 7. The rate of hypochlorous acid decomposition goes through a minimum in the pH 9–10 region. The rate begins to increase above pH 10, and correspondingly, the formation of ClO_2^- also increases. Thus, the ClO_2^- intermediate postulated by Lister[16,17] has been measured directly in the high pH region. In light of this fact, an experiment was carried out to determine if ClO_2^- could be detected in a decomposing hypochlorous acid solution at lower pH values. The initial concentration of hypochlorous acid was 0.0233 M and the initial pH was 7.1. Flow injection analysis was used to measure the ClO_2^- concentrations in the partially decomposed samples. The partially decomposed solutions showed 19, 29, and 35% decomposition. No ClO_2^- could be detected. This corresponds to a maximum ClO_2^- concentration of $\leq 3.0 \times 10^{-7}$ M. Thus, the ClO_2^- present is ≤0.008% of the total HOCl present at the beginning of the decomposition.

Temperature and Medium Effects. The decomposition of hypochlorous acid was studied at 15, 25, 35, 40, and 50 °C. The

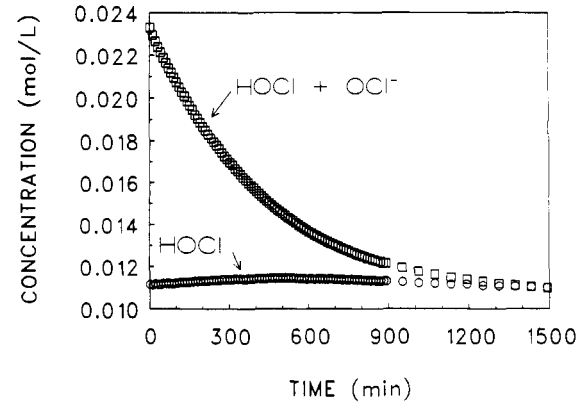

Figure 5. Plot of concentration vs time for total [HOCl] + [OCl^-] and also for [HOCl] alone. Conditions: initial pH = 7.1, 50 °C.

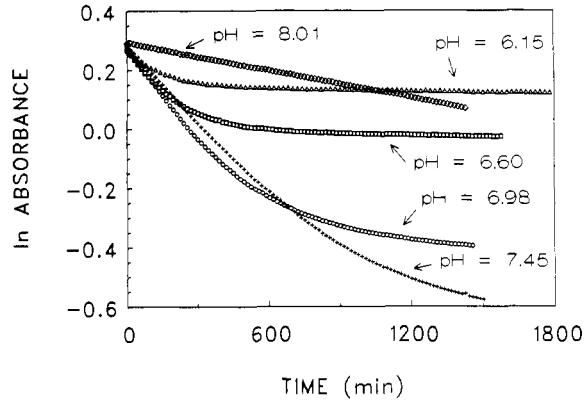

Figure 6. Plot of ln absorbance of hypochlorous acid vs time for five kinetic experiments at different initial pH values. Conditions: C^{i}_{HOCl} = 0.02333 M, 1-cm cell, 50 °C, and 254.7 nm.

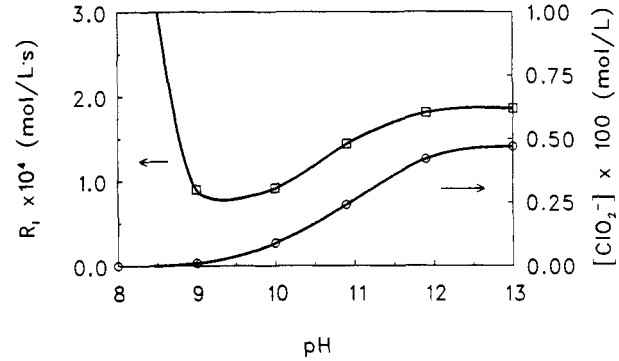

Figure 7. Plot of the rate of disappearance of (HOCl + OCl^-) and the rate of formation of ClO_2^- after 25% decomposition vs pH. $R_i = (C^{i}_{HOCl} - C^{t}_{HOCl})/t$. The data point at 7.07 × 10^{-4} M/s and pH 8 is off scale. Conditions: C^{i}_{HOCl} = 0.15 M, 0.5 M borate buffer, and 90 °C.

experimental rate constants were obtained from linear third-order plots by the equation

$$k_{exp} = \epsilon^2\{slope\}(1 + K_a/[H^+])^2(1 + [H^+]/K_a)/6$$

The values obtained for k_{exp} are (4.90, 12.5, 31.3, 46.6, and 97.2) × 10^{-3} M^{-2} s^{-1}, respectively. (The experimental conditions were such that the ratio of $K_a/[H^+]$ = 0.5 and was constant for each experiment. C^{i}_{HOCl} = 0.0233 M.) The 25 °C value of 12.5 (in a medium of 1 M $NaClO_4$) for k_{exp} is bracketed by the literature values of 26.3 (4 M NaCl)[3] and 9.14 (no controlling electrolyte).[2] The differences in these values are primarily attributed to the vast differences in the controlling electrolyte employed. The measured activation parameters are $\Delta H^{\ddagger}$ = 64.0 ± 0.6 kJ/mol and $\Delta S^{\ddagger}$ = −67 ± 2 J/mol K. The value for $\Delta H^{\ddagger}$ is in good agreement with the value of 67.4 kJ/mol obtained by Yokoyama and Takayasu.[3]

Table II. Comparison of the Initial Rates of Decomposition of HOCl in 1.0 M $NaClO_4$ in the Solutions Shown[a]

buffer or Cl^-	$C_{buffer\ or\ Cl^-}$ (M)	initial rates of decomposition 5%	10%	15%
no buffer	0.0	2.8	2.8	2.6
phosphate	0.0704	3.0	3.0	2.9
carbonate	0.0704	2.8	2.4	2.2
borate	0.352	2.6	2.1	2.0
phosphate[b]	0.352	4.5	4.4	4.1
phosphate[b]	0.352	4.6	4.5	4.0
acetate	0.352	3.7	3.6	3.3
chloride[b,c]	0.352	4.0	3.9	3.6
chloride[b,c]	0.352	4.2	4.0	3.7

[a] Conditions: C_{HOCl} = 0.0233 M, pH = 7.10, 50 °C, and initial rate = $(\Delta Abs/\Delta t) \times 10^5$ (s^{-1}). [b] Replicate experiments. [c] Total ionic strength is 1.0 M.

The effect of several buffer solutions on hypochlorous acid decomposition at 50 °C was studied. The rate of decomposition of buffered hypochlorous acid solutions is compared to the rate of decomposition of unbuffered hypochlorous acid in Table II. Even though 0.0233 M hypochlorous acid is a buffer system itself, it has a low buffer capacity and the pH begins to change dramatically after 15% decomposition. On the basis of this fact, only the initial rates at 5, 10, and 15% decomposition of hypochlorous acid were used for the comparison.

The effect of dilute (0.0704 M) concentrations of phosphate and carbonate on the initial rate of decomposition as compared to the unbuffered hypochlorous acid solution is small and cannot be distinguished from the experimental error involved (±5%). In addition, the use of borate buffer resulted in a small decrease in the initial rate. The acetate buffer increased the initial rate of decomposition by a factor of 1.3. The replicate experiments using 0.352 M phosphate buffer compared to the unbuffered solutions show that the initial rate is almost doubled. These changes in the initial rate of decomposition could be an ionic strength effect caused by the high concentration of buffer present. Another possibility is a medium effect in which the buffer changes the way the species involved interact with each other. In any case, the conclusion is, if a buffer solution must be used in similar systems for future work, dilute phosphate or carbonate buffers would be preferred due to the fact that they do not effect the initial rate of decomposition and also have pK values in the neutral pH region.

The effect of 0.352 M chloride ion in 0.648 M $NaClO_4$ upon the reaction rate was also studied (Table II). The initial rates of these experiments are increased by a factor of 1.4 as compared to the unbuffered reaction. In this case, the ionic strength is the same as the unbuffered experiment. The increased rate appears to be caused either by a shift in the hydrolysis of Cl_2 initiated by Cl^- or a medium effect caused by differences in the Cl^- and ClO_4^- ions. As a result of these comparisons it is clear that caution must be taken when comparing literature data for hypochlorous acid decomposition at different ionic strengths and in different media.

Mechanistic Detail. The observed third-order kinetics and pH dependence suggest a fast initiation step between two HOCl molecules (or HOCl and OCl^-). The third OCl^- (or HOCl) reacts in the second, or perhaps a later step, which is rate-determining. The first step cannot be rate-determining because second-order kinetics would be observed. While any other step can be rate-determining, there is another requirement. Each reaction preceding the rate-determining step must be in a preequilibrium and must be characterized by a relatively small equilibrium constant. If this were not the case, at least one of the intermediate products would accumulate in the system. The presence of intermediate species could not be detected.

If the initial reaction were a simple oxygen transfer between two HOCl molecules, the product would be ClO_2^- (after subsequent deprotonation). However, ClO_2^- quickly reacts with the excess HOCl producing ClO_3^- and perhaps ClO_2. In this case, the mechanism would be consistent with second-order kinetics and the possibility can be rejected. Furthermore, no ClO_2 formation was detected spectrophotometrically.

The following proposed mechanism is based on the observed rate law, stoichiometry and other experimental observations for HOCl decomposition in the neutral pH region. The associated rate constants given correspond to 50 °C.

$$2HOCl = Cl_2O{\cdot}H_2O \qquad K_1 = 0.030\ M^{-1} \tag{13}$$

$$OCl^- + Cl_2O{\cdot}H_2O \rightarrow HOCl + HCl_2O_2^- \qquad k_2 = 3.0\ M^{-1}\ s^{-1} \tag{14}$$

$$HCl_2O_2^- = HClO_2 + Cl^- \tag{15}$$

$$HOCl + Cl_2O{\cdot}H_2O \rightarrow HOCl + H_2Cl_2O_2 \qquad k_4 = 3.6 \times 10^{-3}\ M^{-1}\ s^{-1} \tag{16}$$

$$H_2Cl_2O_2 = HClO_2 + Cl^- + H^+ \tag{17}$$

$$HClO_2 = ClO_2^- + H^+ \tag{18}$$

$$ClO_2^- + Cl_2O{\cdot}H_2O \rightarrow HOCl + HCl_2O_3^- \qquad k_7 \geq 6 \times 10^4\ M^{-1}\ s^{-1} \tag{19}$$

$$HCl_2O_3^- = HClO_3 + Cl^- \tag{20}$$

$$HClO_3 = ClO_3^- + H^+ \tag{21}$$

$$HOCl = OCl^- + H^+ \qquad K_{10} = 6.41 \times 10^{-8}\ M \tag{22}$$

$$Cl_2 + H_2O = HOCl + Cl^- + H^+ \tag{23}$$

$$k_{11} = 1.2 \times 10^1\ s^{-1}$$

$$k_{-11} = 1.6 \times 10^5\ M^{-2}\ s^{-1}$$

The value of K_1 was estimated from ΔH^* of the Cl_2O hydrolysis reaction.[18] The values of k_2 and k_4 were experimentally determined in this work. The minimum value of k_7 was estimated in this work by the fact that no ClO_2^- could be detected during the reaction. This is consistent with a related study[4] where HOCl was assumed to react with ClO_2^- with a rate constant of $2.1 \times 10^3 \pm 0.1$ (25 °C). Therefore, by substitution of the Cl_2O hydrolysis reaction into their equation, k_7 can be calculated to be 2×10^5 at 25 °C. The values of k_{11} and k_{-11} are estimated from literature data for the equilibrium constant[19] and the forward rate constant.[20] The equilibrium constant for HOCl at 50 °C was determined in this work.

Reaction 13 is proposed to be the initial step in the decomposition mechanism, which can be visualized as follows:

(18) Beach, M. W.; Margerum, D. W. *Inorg. Chem.* **1990**, *29*, 1225–1232.
(19) White, G. C. *Handbook of Chlorination*, Van Nostrand Reinhold Co.: New York, 1972; p 183.
(20) Aieta, E. M.; Roberts, P. V. In *Water Chlorination Chemistry: Environmental Impact and Health Effects*; Jolley, R. L.; Bull, R. J.; Davis, W. P.; Katz, S.; Robert, M. H., Jr.; Jacobs, V. A., Eds.; Lewis Publishers Inc.: Chelsea, MI, 1984; Vol. 5, p 786.

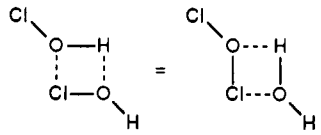

The product of eq 13 is represented as a partially solvated chlorine monoxide adduct. Reaction 14 is a rate-determining step involving the oxidation of OCl^- by the partially solvated Cl_2O to form an $HCl_2O_2^-$ intermediate which is a postulated intermediate in the decomposition of chlorous acid.[21] This step may occur by the following push–pull transition:

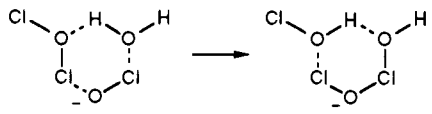

This scheme is very similar to the previous one through the involvement of one solvent molecule in the transition state. Recently, similar reaction schemes have been proposed.[18,22,23] In Cl_2O, there is a partial negative charge on the oxygen atom. Thus, this oxygen atom should readily hydrogen bond with a solvent molecule. In OCl^-, the negative charge is located predominantly on the oxygen. Therefore, the interaction between this oxygen atom and the partially positive charged oxygen atom of Cl_2O is also reasonable. A similar interaction can also be envisioned between the chlorine atom of OCl^- and the oxygen from water. The proposed six-membered ring is expected to be favorable.

In the proposed transition state, the rearrangement of the chemical bonds may be induced by either a H^+ transfer from H_2O to Cl_2O or a Cl^+ transfer from Cl_2O to OCl^-. In both cases, the reaction leads to the formation of HOCl and $HCl_2O_2^-$. The $HCl_2O_2^-$ intermediate is expected to undergo fast dissociation (eq 15) to form $HClO_2$ and Cl^-. Under the applied conditions, the deprotonation of chlorous acid (eq 18) is extremely rapid. Reaction 16 is a rate-determining step, in parallel with reaction 14, involving the oxidation of HOCl by Cl_2O. The mechanistic considerations for eqs 14 and 15 also apply to eqs 16 and 17. The negative charge on the oxygen atom of HOCl is substantially smaller than that in OCl^-. Therefore, the interaction between HOCl and Cl_2O must be weaker, resulting in a significantly slower reaction.

Reaction 19 is the oxidation of ClO_2^- by Cl_2O for which a reaction scheme similar to that given above can be envisioned:

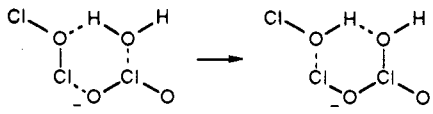

Even though ClO_2^- can also be oxidized by HOCl by a different pathway[24] involving the formation of Cl_2O_2, the reaction between ClO_2^- and Cl_2O is preferred. Approximately 3% Cl_2O is present at 50 °C in an aqueous solution of HOCl. Therefore, Cl_2O is formed in at least 4–5 orders of magnitude higher concentration than Cl_2O_2. In order to be competitive, Cl_2O_2 would have to be much more reactive than chlorine monoxide.

Reactions 20 and 21 follow as fast steps to produce the observed final ClO_3^- product. As the decomposition proceeds, the H^+ produced in eqs 17, 18, 20, and 21 rapidly converts OCl^- to HOCl (eq 22). In addition, as the pH becomes acidic (pH ≤ 3), HOCl is converted to Cl_2 in a side reaction shown in eq 23.

Indirect evidence for the mechanism presented above and the role of Cl_2O can be taken from Figure 7. The rate of decomposition of hypochlorous acid at 90 °C in alkaline solution has two maxima. One maximum occurs at pH 13, and the other occurs below pH 8. The rate of decomposition at pH 8 is 10 times faster than the rate at pH 9–10, which is the rate minimum, and four times faster than the rate at pH 13. This suggests that the decomposition pathway, and hence the mechanism, is changing in this pH region. At pH 10 or above, there is essentially no HOCl present, and for this reason virtually no Cl_2O can form by means of eq 13. Consequently, ClO_2^- begins to build up in the system because reaction 19 is no longer available and ClO_2^- must form ClO_3^- by a slower alternative process. Thus, it is not surprising that in very alkaline solution OCl^- decomposes by a different mechanism since no ClO_2^- can be detected below pH 9. As the pH decreases below 9, HOCl is formed and the rate of decomposition again increases due to the proposed pathway available involving Cl_2O.

Table III. Calculation of k_{exp} and k_2 using Third-Order Rate Law and Data for 5% Decomposition[a]

pH_i	$rate_i$ ($M\ s^{-1}$)	k_{exp} ($M^{-2}\ s^{-1}$)	k_2 ($M^{-1}\ s^{-1}$)
6.15	8.17E–08	0.0948	3.16
6.35	1.09E–07	0.0915	3.05
6.60	1.36E–07	0.0844	2.81
6.72	1.40E–07	0.0790	2.63
6.86	1.65E–07	0.0879	2.93
6.98	1.62E–07	0.0870	2.90
7.09	1.61E–07	0.0910	3.03
7.29	1.30E–07	0.0909	3.03
7.44	1.09E–07	0.0997	3.32
7.61	7.42E–08	0.1008	3.36
7.73	4.45E–08	0.0848	2.83
8.01	1.97E–08	0.0971	3.24
	av	0.090_7	3.0_2
	±	0.006_3	0.2_1

[a] Conditions: C^i_{HOCl} = 0.0233 M, 50 °C.

The experimental determination of k_2 and k_4 is dependent upon the integrity of the steady-state approximation.

The experimental observations indicate that the reaction of $Cl_2O{\cdot}H_2O$ with OCl^- is nearly 1000 times faster than with HOCl. Thus, if the pH is ≥6, eq 24 can be rewritten in the following simplified form:

$$d[ClO_3^-]/dt = \frac{k_1k_2[HOCl]^2[OCl^-]}{k_{-1} + k_2[OCl^-]} \qquad (25)$$

Since the maximum OCl^- concentration of any of the experiments in this work is 0.023 M, it is reasonable to assume that $k_{-1} \gg k_2[OCl^-]$ (k_{-1} = 10.8 s^{-1}, 25 °C). Elimination of the $k_2[OCl^-]$ term gives the following rate law, which is equivalent to the experimentally determined rate law given by eq 8:

$$d(ClO_3^-)/dt = (k_1k_2/k_{-1})[HOCl]^2[OCl^-] \qquad (26)$$

By using eq 26, k_2 was evaluated directly from the experimental data at 50 °C by the following relationship: $k_1k_2/k_{-1} = k_{exp}$. Tables III and IV give the values of k_2 calculated from k_{exp} for each kinetic experiment carried out at different pH values. In Table III, k_{exp} is calculated using the derived third-order rate law. The initial pH of each experiment was used to determine the individual concentrations of HOCl and OCl^-. In Table IV,

(21) Kieffer, R. G.; Gordon, G. *Inorg. Chem.* **1968**, *7*, 239–244.
(22) Yiin, B. S.; Margerum, D. W. *Inorg. Chem.* **1990**, *29*, 1942–1948.
(23) Yiin, B. S.; Margerum, D. W. *Inorg. Chem.* **1990**, *29*, 2135–2141.
(24) Tachiyashiki, S.; Gordon, G. *Environ. Sci. Technol.* **1991**, *25*, 468–474.

Table IV. Calculation of k_{exp} and k_2 from Derivative of First-Order Rate Law and Data for 5% Decomposition with Experimental Parameters the Same as Table III.

pH_i	$\ln (A_0/A_t)t$ (s^{-1})	k_{exp} (M^{-2} s^{-1})	k_2 (M^{-1} s^{-1})
6.15	1.10E-05	0.0993	3.31
6.35	1.43E-05	0.0933	3.11
6.60	1.82E-05	0.0878	2.93
6.72	1.88E-05	0.0824	2.75
6.86	2.21E-05	0.0916	3.05
6.98	2.16E-05	0.0900	3.00
7.09	2.13E-05	0.0936	3.12
7.29	1.45E-05	0.0789	2.63
7.44	1.20E-05	0.0849	2.83
7.61	9.69E-06	0.1024	3.41
7.73	5.81E-06	0.0861	2.87
8.01	2.59E-06	0.0994	3.31
	av	0.090_8	3.0_3
	±	0.007_0	0.2_4

the values of k_2 and k_{exp} were calculated using eq 12 which assumes that the initial decomposition is first-order in OCl^-.

Below pH 4, the $k_4[HOCl]$ term dominates the $k_2[OCl^-]$ term. Under these conditions the following rate law is derived from the proposed mechanism, while making assumptions analogous to those previously introduced:

$$d[ClO_3^-]/dt = (k_1k_4/k_{-1})[HOCl]^3 \qquad (27)$$

Figure 8 is a plot of (absorbance)$^{-2}$ vs time at an initial pH of 6.15. After the first 1000 min., the solution contains mostly HOCl and essentially no OCl^-. Thus, the slope of the previously mentioned third-order plot should be proportional to k_4 as described by eq 27. The value of k_4 is equal to 0.0036 ± 0.0003 M^{-1} s^{-1}.

Comparison of eq 3 observed by Yokoyama and Takayasu[3] and eq 25 shows that these rate equations are equivalent. If every term in eq 25 is divided by k_{-1}, the following equation is obtained:

$$d[ClO_3^-]/dt = \frac{(k_1k_2/k_{-1})[HOCl]^2[OCl^-]}{1 + (k_2/k_{-1})[OCl^-]} \qquad (28)$$

Here $k_1k_2/k_{-1} = a$ and $k_2/k_{-1} = b$ in eq 3. At the OCl^- concentration in the current work (≤0.023 M), the k_2/k_{-1} $[OCl^-]$ term can be neglected to produce the simple third-order rate law in eq 26. At Yokoyama and Takayasu's initial concentration of 0.18 M OCl^-, the term in the denominator of eq 28 should not be neglected. Thus, the mechanism proposed here agrees with their experimentally observed rate expression.

Simulations. Numerical simulation was used to test the proposed mechanism and the experimentally determined rate constants (k_2 and k_4) in terms of their ability to simulate the experimental data. Also, an attempt was made to correct for any deviation obtained from this simulation by adjusting the k_2 and k_4 parameters. The iterative technique used is the GEAR algorithm.[25] While equilibrium constants alone cannot be used directly in the simulation technique, it was found that the results obtained were dependent only upon the magnitude of K_1 (eq 13) and not on the individual values of k_1 or k_{-1}.

The experimental and simulated data were obtained under the following conditions: C^i_{HOCl} = 0.0233 M, initial pH = 7.10, and 50 °C. The total decomposition of hypochlorous acid was 50% with a reaction time of 24.5 h. By using our experimental values of k_2 and k_4, the simulated curve of absorbance vs time demonstrates a good fit of the experimental data. After several hundred minutes, the simulated curve shows a 10% deviation from the experimental data. The major source of error in the fit achieved is most likely due to error in the determination of k_4. Fitted values for the rate-determining steps were obtained by minimizing the deviation in the y-axis through systematic adjustment of the values of k_2 and k_4.

(25) Peintler, G. *Zita Program Package for the Fitting of Parameters in Kinetic Models of Reaction Mechanisms*; Version 2.1; Institute of Physical Chemistry, JATE: Szeged, Hungary, 1990, and personal communication.

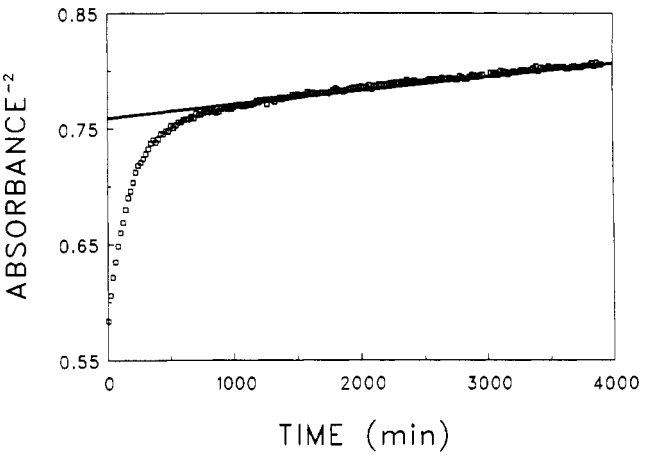

Figure 8. Plot of (absorbance)$^{-2}$ of hypochlorous acid vs time at an initial pH of 6.15, C^i_{HOCl} = 0.0233 M, 50 °C, and 1-cm cell.

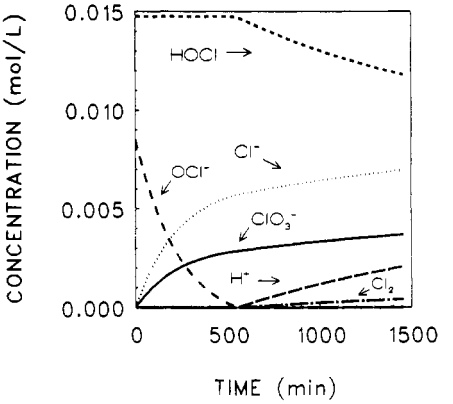

Figure 9. Simulated concentration of observable species in the proposed mechanism as a function of time using fitted values of k_2 and k_4. Experimental conditions are as follows: C^i_{HOCl} = 0.0233 M, initial pH = 7.1, 50 °C, and 1-cm cell.

The experimental and fitted values are as follows:

$$k_2(\text{experimental}) = 3.0 \pm 0.2\ M^{-1}\ s^{-1}$$

$$k_4(\text{experimental}) = 0.0036 \pm 0.0003\ M^{-1}\ s^{-1}$$

$$k_2(\text{fitted}) = 3.0 \pm 0.2\ M^{-1}\ s^{-1}$$

$$k_4(\text{fitted}) = 0.0045 \pm 0.0006\ M^{-1}\ s^{-1}$$

The experimental and fitted values of k_2 are identical. Although there is a small difference in the experimental and fitted values of k_4, the values are statistically indistinguishable. On the other hand, if the simulation is carried out without the parallel rate-limiting step involving HOCl (eq 16), the simulated curve of absorbance vs time flattens out after a few hundred minutes in contrast to experimental data. Due to the conversion of all of the OCl^- to HOCl during the decomposition, the simulated curve and the experimental data cannot converge in the later part of the decomposition because, in this case, the simulation lacks an available pathway for decomposition. This difference between the simulation and the experimental data was observed even when the value of k_2 was increased by several orders of magnitude. Thus, the simulation supports the proposed parallel rate-determining steps.

By using the fitted values of k_2 and k_4, the concentration of all species present in the system were calculated.[25] The con-

centration of each abundant species is shown vs time in Figure 9. This simulation does show the expected trend in each concentration. The proposed intermediate species are all present in small ($\leq 3 \times 10^{-6}$ M) and relatively constant concentrations. Thus, the simulation supports the steady-state assumption applied to these species in the derivation of the rate law.

The presence of Cl_2 is evident in the later portion of the simulated decomposition. This is due to the increasing Cl^- and H^+ concentrations shifting the equilibria of the Cl_2 hydrolysis reaction (eq 23) to form more Cl_2. The Cl_2 present after 750 min of decomposition is 1% of the HOCl concentration and is nearly 4% of the HOCl concentration at 1500 min. This chlorine formed in the decomposition reaction mixture could be involved in other decomposition pathways involving Cl_2 directly. Lastly, it is important to note that the Cl_2 is formed in relatively acidic solution ($pH \leq 3$) and no appreciable Cl_2 concentration is observed by the simulation in the pH 5–8 range.

Supplementary Material Available: Text discussing the calculation of pK_a for Table S1 and a listing (Table S1) of the data used to calculate pK_a (2 pages). Ordering information is given on any current masthead page.